Journal of Applied Physics

Electrical behavior of YBa2Cu3O7−x grain boundary junctions under low magnetic field

S. Nicoletti and J.-C. Villegier

Citation: J. Appl. Phys. 82, 303 (1997); doi: 10.1063/1.366280
View online: http://dx.doi.org/10.1063/1.366280
View Table of Contents: http://jap.aip.org/resource/1/JAPIAU/v82/i1
Published by the American Institute of Physics.

Electrical behavior of $YBa_2Cu_3O_{7-x}$ grain boundary junctions under low magnetic field

S. Nicoletti[a)]
CNR-Istituto LAMEL, via Gobetti 101, I-40129 Bologna, Italy

J.-C. Villegier
DRFMC/SPSMS-CEA Grenoble, F-38054 Grenoble Cedex 09, France

(Received 22 November 1996; accepted for publication 27 March 1997)

The characterization of high temperature superconductor grain boundary junctions under a magnetic field in the mT range is reported. The devices were obtained by patterning narrow stripes in a $YBa_2Cu_3O_{7-x}$ (YBCO) film deposited on $SrTiO_3$ and MgO symmetric bi-crystal substrates. To allow the investigation of devices having different current density, two grain boundary disorientations were considered: 24° and 45° for $SrTiO_3$ and 24° for MgO. Current-voltage characteristics as a function of the applied field for several temperatures have been collected. The experimental data are discussed on the basis of the electrical parameters obtained for the different substrates. The periodic modulation of the Josephson critical current with the magnetic field indicates that the behavior of YBCO grain boundary junctions can be approximated by the standard overlap junctions model. A comparison between the experimental variation of the critical current with theoretical behavior allows for the determination of the current density distribution in the grain boundary as a function of the ratio of the largest junction dimension L and the Josephson penetration depth λ_J. The nature of the barrier and the transport mechanism across the grain boundary is, therefore, investigated; good agreement between the experimental results and the expected behavior of a superconductor-insulator-superconductor structure where the barrier is intrinsically defective is observed. © *1997 American Institute of Physics.* [S0021-8979(97)03213-1]

I. INTRODUCTION

In high temperature superconducting materials, large angle grain boundaries (GBs) behave like a weak link with resistively shunted junction (RSJ) behavior.[1] Despite the large amount of studies carried out on this behavior in the last few years, the mechanism underlying transport in the GB is still under debate and still not fully understood.

From the microscopic point of view, several authors have pointed out that the structure of a $YBa_2Cu_3O_{7-x}$ (YBCO) film close to the GB consists of a network of dislocations at the nm scale while the macroscopic boundary is a sequence of three-dimensional (3D) facets having typical dimensions of 10–100 nm.[2–4] The morphology of the GB interface is commonly attributed to the island-growth mechanism. The dislocation network forms to compensate the mismatch at the interface during the mutual coordination. However, in the limit of the investigation techniques currently available, no impurity phases have been found to date. Since a normal-conducting phase is absent in the phase-diagram of YBCO, the interface of the GB cannot be associated with either an insulator or a normal-conductor or a semiconductor barrier.

To explain the electrical behavior of this kind of structure, two main models have been proposed: the defective insulating barrier model, hereafter referred to as an superconductor-insulator-semiconductor (SI*S) structure, at the GB interface proposed by Gross *et al.*[5,6] and the two channel model of Moeckley *et al.*[7] and by Sarnelli.[8] The basic assumption of the former model is the existence of a thin insulating layer. The lack of uniformity as well as density of the localized states in the barrier can account for the observed experimental data. On the other hand, the two channel model assumes that the interface between the grains consists of a sequence of superconducting and normal channels. This channel network can either be randomly distributed[7] or pinned onto a defective network.[8] In both cases, the GB is intrinsically shunted and the junctions are strongly overdamped.

The combined effect of the faceting and of the $d_{x^2-y^2}$ space symmetry of the wave form describing the superconducting state on the transport properties has been discussed by Copetti *et al.*[9] and by Hilgenkamp *et al.*[10] They showed that a considerable part of the reduction of critical current of a GB junction can be attributed to the simultaneous occurrence of these phenomena and the particular case of a 45° asymmetric GB is discussed therein. The non-Fraunhofer-like dependence of the Josephson critical current under a magnetic field in small junctions can be explained by the occurrence of facetting and the space symmetry, simultaneously.[10]

Furthermore, the role of random occurring defects inside the barrier on the electrical behavior of a conventional SI*S junction under magnetic field was recently discussed by Itzler *et al.*[11] They showed that columnar defects induced in the barrier act as pinning centers for the Josephson vortices. The presence of these vortices significantly change the Josephson current distribution and, therefore, the electrical behavior of the device.

[a)]Electronic mail: nicoletti@area.bo.cnr.it

The main focus of this work is the characterization of YBCO grain boundary junctions fabricated on $SrTiO_3$ and MgO symmetrical bi-crystal substrates. For each sample, we have collected the current-voltage (I-V) characteristics under a magnetic field (H) in the mT range, at various temperatures. The obtained results are discussed by comparing the experimental data with the expected behavior for different junction configurations as a function of the Josephson penetration depth λ_J. The nature of the barrier and the transport mechanism across the grain boundary is, therefore, investigated.

II. EXPERIMENT

We consider three different samples fabricated on symmetrical bi-crystal substrates: a (001)-oriented MgO substrate with a 24° tilted GB and two (001)-oriented $SrTiO_3$ substrates with 24° and 45° tilted GBs, respectively.[12] To decrease the preferential erosion along the GB, always found to be present in bi-crystal samples,[2] the substrates were carefully repolished before the deposition and the boundary grove was, therefore, reduced to 5 nm. The superconducting film was deposited by the pulsed laser ablation technique; the 180-nm-thick YBCO layer was deposited at 720 °C in 40 Pa O_2 dynamical pressure at a rate of 0.06 nm/s. After the deposition, the samples were slowly cooled in 500 hPa of oxygen. The films were then patterned by a standard photolithographic technique followed by Xe ion milling at 300 eV. After the patterning, we obtained several stripes of different widths onto each sample. A more detailed discussion of the fabrication procedure is reported in our previous papers.[13,14]

The electrical characterization was performed in a double shielded Dewar. The samples were mounted on a cryogenic probe, allowing measurements down to liquid helium temperature. The magnetic field was applied using a small coplanar coil wound around the sample such that the magnetic field was perpendicular to the sample surface and parallel to the macroscopic GB. The I-V characteristics were collected using a fully computer controlled setup. The critical current values, $I_{J,C}$, were evaluated as the current corresponding to a 10 μV voltage drop across the junction.

III. RESULTS AND DISCUSSION

The I-V characteristic has been measured as a function of the applied magnetic field at different temperatures for each sample. Figure 1 shows the temperature dependence of the Josephson critical current $I_{J,C}$ for each series of junctions considered here; the values are scaled with respect to the critical temperature, T_C, and the critical current at $T=0$ K, $I_{J,C,T=0\ \mathrm{K}}$. Since all of the samples exhibit a similar behavior, we conclude that the basic transport mechanism is intrinsic to the GB and is not affected by either the disorientation angle or by the misfit with respect to the substrate material. Consequently, the discussion of the results will be focused mainly on the transport behavior, regardless of the structural properties of each GB. Figure 1 also shows the theoretical behavior obtained under the assumption of an SI*S junction

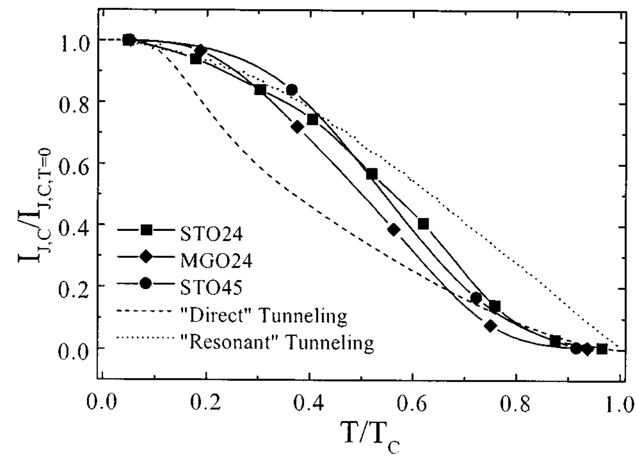

FIG. 1. Temperature dependence of Josephson critical current for junctions fabricated on (■) 24° $SrTiO_3$, (◆) 24° MGO, and (●) 45° $SrTiO_3$ bi-crystal samples. The values are scaled with respect to T_C and $I_{J,C,T=0\ \mathrm{K}}$. The dashed and the dotted lines show, respectively, the theoretical behavior for ''direct'' and ''resonant'' tunneling transport mechanisms through a defective insulating barrier.

barrier for two different transport mechanisms through this type of barrier. Their relevance on the results presented here will be discussed later.

Under magnetic field, the total Josephson current of a given junction is strongly dependent on the Josephson penetration depth λ_J and on the applied field itself. In a uniform junction, two reference behaviors can distinguished as a function of λ_J.[15] If the junction dimensions are small in comparison with λ_J, then the magnetic field inside the junction is constant and equal to the applied field, while the phase shows a linear space variation along the barrier. The current density is periodically modulated, giving the typical Fraunhofer-like behavior of I_C as a function of H. On the contrary, if λ_J is smaller than the junction dimensions, then the field self-generated by the bias current is non-negligible. The magnetic field inside the junction differs from the applied field by the contribution from the self-field and the phase variation is no longer linear along the barrier. Consequently, the current distribution $J(x)$ is modulated by both the self-field and the applied field.

In our case, the magnetic field was applied parallel to the macroscopic GB and perpendicular to the largest junction dimension, that is, the size L of the patterned stripe. Hence, we can analyze the behavior of the GB junctions under a magnetic field by comparing the electrical measurements as a function of the ratio L/λ_J. Table I shows the significant parameters for each set of junctions at various temperatures. The λ_J values were calculated by taking the values recently measured by de Vaulchier *et al.*[16] for the London penetration depth λ_L. In view of these results, we can analyze the behavior of the GB junctions in the different regimes $L/\lambda_J \lessgtr 1$ by comparing the 5 μm large junctions fabricated on the different samples.

In Fig. 2 we report the I-V characteristics as a function of the applied magnetic field H taken for the junction fabricated on the 45° $SrTiO_3$ sample at 4.2 K. Since λ_J is 3.4 μm for this sample, a Fraunhofer-like diffraction pattern of the

TABLE I. Electrical parameters of the junctions fabricated on the three different substrates at various temperatures.

Substrate	T (K)	$J_{J,C}$ (A/cm^2)	$R_N \cdot A$ ($\Omega\ \mu$m^2)	$I_{J,C}R_N$ (μV)	λ_J (μm)
	4.2	6.6×10^3	3.0	221	3.4
$SrTiO_3$	30	6.1×10^3	2.9	193	3.5
45° bi-crystal	60	1.1×10^3	2.5	31	7.4
	77	3.8×10^1	2.5	1.1	-
	4.2	1.0×10^5	0.44	440	1.1
MgO	30	7.4×10^4	0.44	326	1.2
24° bi-crystal	60	8.0×10^3	0.44	35	2.7
	77	4.9×10^2	0.44	2.2	-
	4.2	3.3×10^5	0.56	1848	0.48
$SrTiO_3$	30	2.5×10^5	0.55	1375	0.54
24° bi-crystal	60	9.2×10^4	0.57	524	0.83
	77	1.0×10^4	-	~56	-

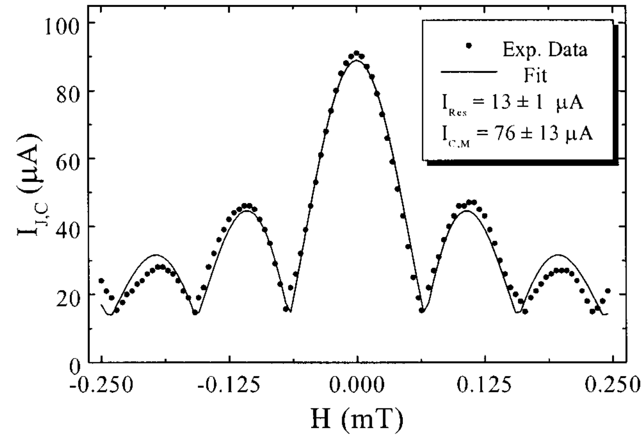

FIG. 3. Comparison of the $I_{J,C}$ vs H data of Fig. 2 (●) and the simulated curve obtained with the assumption of a nonuniform current density distribution as given by (1) (solid line). The parameters of the simulation are reported in the inset.

Josephson current is expected for this junction. We always observe two different phenomena, even at higher temperature. The Josephson critical current $I_{J,C}$ is modulated periodically by the magnetic field with the appearance of well defined minima and maxima as a function of H. However, even when the $I_{J,C}$ reach the minima, we still observe a nonvanishing Josephson current. The intensity of the satellite maxima are clearly more pronounced than those expected for a small uniform junction. To evaluate the residual current, the $I_{J,C}$ vs H curve was simulated by considering a nonuniform current density distribution over the barrier, given by the formula:[15]

$$J(x)=J_0\,\frac{\cosh(\kappa x)}{\cosh(\kappa L/2)}, \tag{1}$$

where J_0 is the maximum current density, L is the largest junction size, and κ is a parameter accounting for the nonuniformity in the device. The analytical formula for the Josephson current flowing in the junction is, therefore, given by:[15]

$$I\left(\frac{\Phi}{\Phi_0},\kappa\right)=I_{\mathrm{Res}}+I_{\mathrm{C,M}}\times\frac{\kappa^2}{\kappa^2+\left(\pi\dfrac{\Phi}{\Phi_0}\right)^2}\times\left|\frac{\pi\dfrac{\Phi}{\Phi_0}\sin\left(\pi\dfrac{\Phi}{\Phi_0}\right)}{\kappa\,\tanh(\kappa)}+\cos\left(\pi\frac{\Phi}{\Phi_0}\right)\right|, \tag{2}$$

where the ratio Φ/Φ_0 is the magnetic field given in quantum flux units Φ_0. Figure 3 presents these results along with the experimental data. The dashed line represents the best fit obtained under the hypothesis of a residual current I_{Res} either constant or slightly dependent on H, when H is in the mT range. The parameters of the simulation are reported in the inset. It is worth noting that the $I_{J,C}$ vs H curves obtained for this sample at 30 and 60 K follow a similar behavior to that reported in Figs. 2 and 3, giving a modulation period nearly independent of the temperature.

The different $I_{J,C}$ values as a function of H for a junction fabricated on the 24° MgO sample at 4.2, 30, and 60 K are shown in Fig. 4. Since, λ_J changes from 1.1 μm at 4.2 K

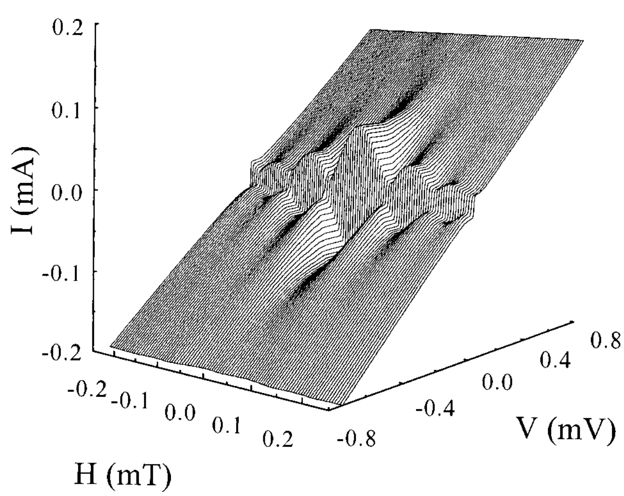

FIG. 2. I-V characteristics vs the applied magnetic field H taken on 5-μm-wide junction fabricated on a 45° $SrTiO_3$ bi-crystal sample at 4.2 K.

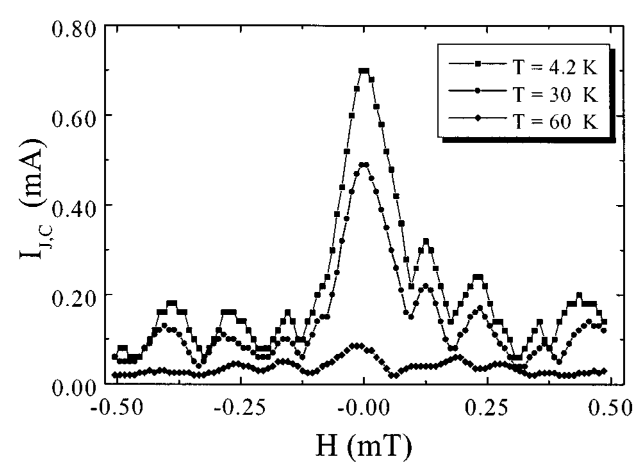

FIG. 4. Josephson critical current vs applied magnetic field for a 5-μm-wide junction fabricated on a 24° MgO bi-crystal sample at 4.2, 30, and 60 K.

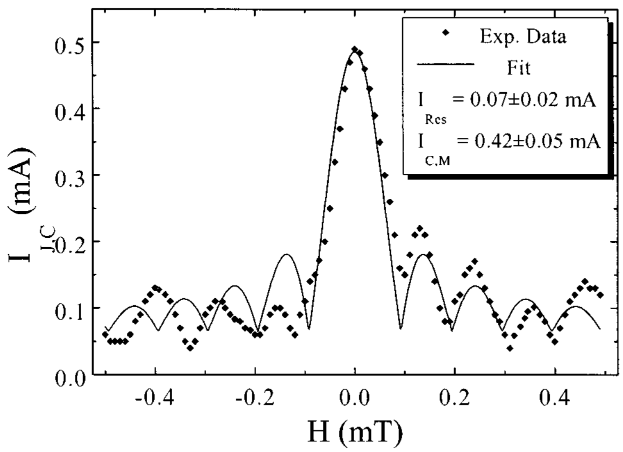

FIG. 5. Comparison of the $I_{J,C}$ vs H data at 30 K for the junction fabricated on 24° MgO bi-crystal sample (◆) and the simulated curve obtained applying the fitting procedure of Fig. 3 (solid line). The parameters of the simulation are reported in the inset.

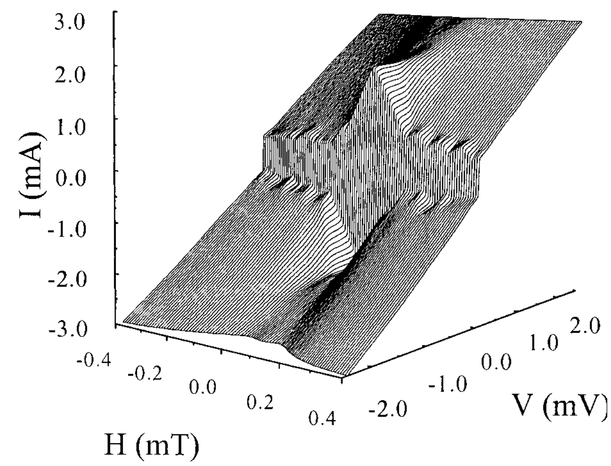

FIG. 6. I-V characteristics vs the applied magnetic field H taken for the junction fabricated on a 24° $SrTiO_3$ bi-crystal sample at 30 K.

to 2.7 μm at 60 K for this junction, we expect a crossover from long junction to small junction behavior by increasing the temperature. However, comparison of the different plots shows that, as the temperature is increased, the curve becomes irregular and asymmetric. The Josephson current is modulated by the magnetic field with the appearance of typical lobes, but at the minima a nonvanishing superconducting current still flows in the junction. At a low temperature, we also observe the slight asymmetry of the I_C pattern while the periodicity as a function of H is quite irregular. This effect was partly screened at lower temperatures, but becomes evident when the temperature increases and the coupling between the carriers is weaker. Figure 5 compares the curve calculated following the previously described fitting procedure with the experimental $I_{J,C}$ vs H data taken at 30 K. The parameters of the simulation are reported in the inset. Even if the periodic modulation is reproduced, the simulation results do not exactly fit the measured curve. However, we observe that the best results were obtained by introducing a bias current I_{Res} either constant or slightly dependent on the magnetic field in the mT range.

Figure 6 display the I-V characteristics taken for different values of H on a junction fabricated on a 24° tilted $SrTiO_3$ bi-crystal at 30 K. As reported in Table I, even at 60 K, $\lambda_J < 1$ μm. The typical periodic modulation of the critical current with the overlap of the adjacent lobes, reported in Fig. 6, agrees well with the behavior of a long junction under a magnetic field expected for this device. Figure 7 compares the experimental data with the theoretical curve calculated following the procedure developed by Pagano *et al.*[17] for long junctions under a magnetic field. We first note that the best fit can be obtained only by considering a current component I_{Res} slightly dependent on H in the examined range. Even if the fitting procedure quite adequately reproduces the period, the amplitude of the modulation is larger than the expected amplitude. The origin of this phenomenon is still unclear. However, for a comprehensive analysis of the $I_C(T)$ and $I_C(H)$ behavior, both the thermal noise influence on the I-V characteristic at high temperature[18] and the possibility of vortex trapping in the electrodes close to the barrier have to be considered. The relevance of these occurrences will be discussed later.

To summarize the experimental data presented in this work, we have observed that the Josephson critical current of the junctions are periodically or quasi-periodically modulated by the applied magnetic field, independent of the GB disorientation. These results are among the best reported to date in the literature. We have also observed that the $I_{J,C}$ do not vanish at the minima, indicating that part of this Josephson current is not modulated by H in the range considered here.

We now discuss the transport mechanism in the barrier. The coexistence of the superconductor and the normal-conductor channels postulated in Refs. 7 and 8 are not consistent with either the uniform decrease of the mean critical current at high field[19] or with the unambiguous periodic modulation of the critical current under low magnetic field observed for our samples. On the contrary, the behavior of our junction can be explained by the assumption of an insulating GB barrier containing a high density of localized states providing the intrinsic shunt for the junction. In fact, if the

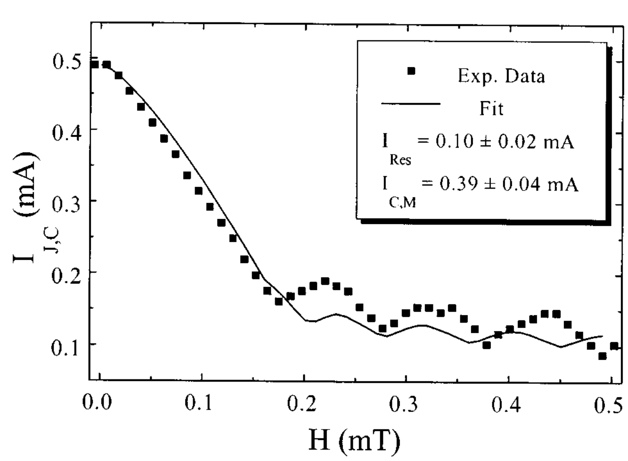

FIG. 7. Comparison of the $I_{J,C}$ vs H data of Fig. 6 (■) and the simulated curve calculated following the procedure described in Ref. 17.

barrier is uniform on the scale of the Josephson penetration depth, then an SI*S structure such as that proposed by Gross *et al.*[5,6] can account for the experimental behavior presented here. Furthermore, the occurrence of electromagnetic resonances in our samples[20,21] indicates the dielectric nature of the grain boundary in such a junction.[22]

The deviations of the $I_{J,C}$ vs H from the Fraunhofer-like dependence has also been ascribed to the mutual occurrence of facetting and $d_{x^2-y^2}$ space symmetry. The facetting has been found to occur at all length scales between the nm and the μm regime. In the frame of the theory discussed in Ref. 10, the effect becomes more prominent as the disorientation angle increases. In particular, in the case of a symmetric 45° tilted GB, the grains will coordinate by mainly facetting the (110) plane and the (100) plane. If we apply the model to this structure, then we obtain a null critical current. The direct observation of this GB morphology was not available since the 45° $SrTiO_3$ sample broke during the experiment. However, this morphology can be assumed similar to those already presented in the literature, that is, with the typical facetting structure over the length of tens of nm.[2–4] By comparing the model with the experimental data, we observe a substantial discrepancy between the results of Ref. 10 and the periodic variations of $I_{J,C}$ measured under a magnetic field for our GB junctions. We can, therefore, conclude that the relevance of the mutual occurrence of facetting and $d_{x^2-y^2}$ space symmetry on the magnetic behavior of the GB junctions, if any, is critically dependent on the facetting plane and is not relevant in our case.

The asymmetric behavior observed for the junctions fabricated on MgO can be explained by considering the vortex pinning. In fact, the intrinsic restraint generated by the substrate-to-film mismatch results in the formation of extended defects even in the GB region. Following the results of Itzler and Tinkham,[11] these defects at the GB interface can explain the strong modifications in the current distribution across the barrier and the presence of Josephson vortex pinned on them can account for the asymmetry in the $I_{J,C}$ vs H curve. On the other hand, due to the large demagnetization factor of a stripe line, the local magnetic field can be higher than the lower critical field $H_{C,1}$ of the electrodes. Under this assumption, Abrikosov vortex stars penetrate the YBCO layer, those in the GB region interacting strongly with the current distribution in the junction. This phenomenon may account for the observed irregularities, particularly when the temperature is high and $H_{C,1}$ is low. However, these irregularities were observed mainly in the MgO samples while the quality of the YBCO films was comparable between the samples (highly textured c-oriented films with $J_C \geqslant 10^6$ A/cm^2 at 77 K). For these reasons, we believe that the asymmetric behavior should be attributed to the presence of Josephson vortex pinned by defects, as discussed in Ref. 11.

We now discuss the occurrence of the residual current under magnetic field in the mT regime. The investigation of the junction behavior under a magnetic field provides information on the current density distribution across the barrier. In particular, as pointed out in Ref. 19, the envelope of the I_C curve measured for H increasing up to several T can be correlated with the conduction mechanism in the barrier; the exponential decay of this envelope provides further evidence of the SI*S nature of the barrier in the GB. However, in the mT range, a perfect periodic Fraunhofer-like $I_{J,C}$ vs H dependence has not been reported to date for YBCO GB junctions and the persistence of a non-negligible Josephson current at the minima has also been reported elsewhere.[23] This behavior, attributed to the intrinsically inhomogeneous and defective nature of the barrier, seems to be a common feature of the high temperature superconducting junctions. However, the former conjecture is no longer valid once the experimental $I_{J,C}(H)$ curve can be correlated with a current density distribution in the device; that is, for example, the case reported in Figs. 3 and 7. Therefore, our results can be explained only in the view of a current component decreasing slightly with the magnetic field. Nevertheless, our results are not exhaustive and further investigations are needed to clarify this occurrence and its nature.

Finally, we discuss the temperature dependence of the Josephson current. We have previously discussed the transport properties of the GB junctions, showing how our data agree with the hypothesis of an intrinsically shunted SI*S barrier. The conduction mechanism in such a barrier has been investigated from a theoretical point of view. While Halbritter[23,24] indicates that the classical tunnel of Cooper pairs across such an intrinsically defective barrier is a main mechanism for conduction, Devyatov and Kupriyanov[25] were able to show that the transport of superconducting carriers can also be accounted for by resonant tunnelling via localized states in the barrier. The temperature variation of the critical current $I_{J,C}(T)$ calculated following the models are presented in Fig. 1 together with the experimental results. The dotted line represents the data obtained by numerical calculation in the case of resonant tunneling for the suppression parameter $\Gamma_{LS}=100$,[26] while the dashed line gives the variation of the I_C as calculated under the hypothesis of ''direct'' tunneling.[24,25] Since neither ''direct'' nor ''resonant'' tunneling can fit the experimental data over the whole temperature range, we cannot discriminate between the proposed transport mechanisms. However, close to zero the data are fitted most accurately by the ''resonant'' tunneling model, while close to T_C the ''direct'' tunneling model gives the more accurate fit. This result suggest that both mechanisms occur simultaneously and, depending on the temperature range, one of them will dominate the conduction process.

IV. CONCLUSIONS

The characterization of YBCO grain boundary junctions fabricated on $SrTiO_3$ and MgO symmetric bi-crystal substrates under a magnetic field in the mT range have been exported. For each sample we have collected the I-V characteristics as a function of the applied magnetic field (H) at various temperatures. The experimental data show that the Josephson critical current is periodically or quasi-periodically modulated by the applied magnetic field, independent of the GB disorientation. The periodic modulations of $I_{J,C}$ by the magnetic field indicate that the behavior of YBCO grain boundary junctions can be approximated by the standard overlap junctions model.

We have deduced the electrical parameters of the junctions fabricated on the different substrates. To obtain the current density distribution in the grain boundary, we have compared the variation of $I_{J,C}$ with the theoretical behavior as a function of the ratio L/λ_J. The additional hypothesis of a Josephson current component dependent slightly on H in the mT range was necessary to fit the experimental curves with the models.

The nature of the barrier and the transport mechanism across the grain boundary has therefore been investigated and good agreement of the obtained results with those expected for an SI*S structure.

ACKNOWLEDGMENTS

This work, partially supported by the ESPRIT Basic Research Project No. 7100, was carried out at DRFMC/SPSMS—CEA Grenoble. S.N. undertook this work in the frame of the CEE-HCM program, project No. ERB4001GT933579. The authors also want to gratefully acknowledge S. Pagano, E. Sarnelli, and B. Ruggiero for supplying the computational tool used in the junction behavior simulation as well as for stimulating discussions. They also acknowledge M. A. Bates for a critical review of this article.

[1] P. Chaudari, J. Manhart, D. Dimos, C. C. Touri, J. Chi, M. M. Oprysko, and M. Scheuermann, Phys. Rev. Lett. **60**, 1653 (1988).
[2] A. Alarco, E. Olsson, Z. G. Ivanov, D. Winkler, E. A. Stepantsov, O. I. Lebedev, A. L. Vasiliev, A. Ya. Tzalenchuk, and N. A. Kiselev, Physica C **247**, 263 (1995).
[3] K. Lee and I. Iguchi, Appl. Phys. Lett. **66**, 769 (1995).
[4] D. J. Miller, T. A. Roberts, J. H. Kang, J. Talvacchio, D. B. Buchholz, and P. H. Chang, Appl. Phys. Lett. **66**, 2561 (1995).
[5] R. Gross and B. Mayer, Physica C **180**, 235 (1991).
[6] R. Gross, L. Alff, A. Beck, O. M. Froehlich, R. Gerber, R. Gerdermann, A. Marx, B. Mayer, and D. Koelle, *2nd Workshop on HTS Applications and New Materials*, edited by D. H. A. Blank (University of Twente Press, The Netherlands, 1995), p. 8.
[7] B. H. Moeckley and R. A. Buhrman, IEEE Trans. Appl. Supercond. **5**, 3414 (1995).
[8] E. Sarnelli, Interface Sci. **1**, 287 (1993).
[9] C. A. Copetti, F. Rüders, B. Oelze, Ch. Buchal, B. Kabius, and J. W. Seo, Physica C **253**, 63 (1995).
[10] H. Hilgenkamp, J. Mannhart, and B. Mayer, Phys. Rev. B **53**, 14586 (1996).
[11] M. A. Itzler and M. Tinkham, Phys. Rev. B **53**, 11949 (1996).
[12] Substrates supplied by Wako Busan, Japan.
[13] J. C. Villegier, H. Moriceau, H. Boucher, R. Chicault, L. DiCioccio, A. Jäger, M. Schwerdtfeger, M. Vabre, and C. Villard, IEEE Trans. Magn. **27**, 1552 (1991).
[14] S. Nicoletti, H. Moriceau, J. C. Villegier, and D. Chateigner, Physica C **242**, 99 (1995).
[15] A. Barone and G.釣Paternó, *Physic and Applications of the Josephson Effect* (Wiley, New York, 1982).
[16] L. A. de Vaulchier, J. P. Vieren, Y. Guldner, L. Bontemps, R. Combescot, Y. Lamaître, and J. C. Mage, Phys. Rev. B **54**, 3482 (1996).
[17] S. Pagano, B. Ruggiero, and E. Sarnelli, Phys. Rev. B **43**, 5364 (1991).
[18] S. K. Tolpygo and M. Gurvitch, Appl. Phys. Lett. **69**, 3914 (1996).
[19] O. M. Froehlich, H. Schulze, A. Beck, B. Mayer, L. Alff, R. Gross, and R. P. Huebener, Appl. Phys. Lett. **66**, 2289 (1995).
[20] S. Nicoletti, thése de doctorat, Universitè J. Fourier, Grenoble 06.06.96, Chap. 5.
[21] A. Beck, A. Strenzel, O. M. Froehlich, R. Gerber, R. Gerdemann, L. Alff, B. Mayer, R. Gross, A. Marx, J. C. Villegier, and H. Moriceau, IEEE Trans. Appl. Supercond. **5**, 2192 (1995).
[22] T. Doderer, Y. M. Zhang, D. Winkler, and R. Gross, Phys. Rev. B **52**, 52 (1995).
[23] See, for example: Y. M. Zhang, D. Winkler, P.-Å Nilsson, and T. Claeson, Phys. Rev. B **51**, 8684 (1995). E. Sarnelli, P. Chaudhari, and J. Lacey, Appl. Phys. Lett. **62**, 777 (1993).
[24] J. Halbritter, Phys. Rev. B **46**, 14861 (1992).
[25] J. Halbritter, Phys. Rev. B **48**, 9735 (1993).
[26] I. A. Devyatov and M. Yu. Kupriyanov, JETP Lett. **59**, 201 (1994).